

Numerical Investigation of the Stress-Strain State of the Curved Pipeline

Viktor A. Rukavishnikov¹, Oleg P. Tkachenko¹, Anna S. Ryabokon¹

¹Computing Center of Far-Eastern Branch, Russian Academy of Sciences, Khabarovsk, Russia,
vark0102@mail.ru
olegt1964@gmail.com
anyuta.riabokon@yandex.ru

Abstract

We investigate three-dimensional mathematical model of the pipeline, which is based on the shells theory by V.Z. Vlasov. A method for the approximate solution of the model equations based on the asymptotic expansion of the solution is proposed. Results of numerical experiments for model problems are given. It is proved that the mathematical model adequately describes the known phenomena of pipelines mechanics. In the numerical experiment, the deplanations of the pipe cross sections were found.

1 Introduction

Presently, the world has begun to work on the development of oil and gas deposits in remote areas. With this development, many new scientific and technical problems have arisen. One of the unsolved problems is the problem of rejection of the pipeline from its design position, see in [1, 2]. Next, the problem arises regarding the study of the dynamics of a pipeline in a deformable medium. A brief review of scientific publications on this topic was made in [3, 4]. In a series of papers [5–9], the kinematics and dynamics of a bent pipeline were investigated, mathematical models were constructed, algorithms for their numerical analysis were developed, and test problems were solved.

Main purposes of this paper are to (1) present a new problem transformation algorithm from three-dimensional to one-dimensional formulation; (2) perform computational experiments on the proposed mathematical model; (3) prove that the mathematical model describes the deplanation of pipe cross sections and (4) determine the displacements of the pipeline for a variable internal pressure difference.

2 Formulation of the Problem

We consider the pipeline of length L with a circular cross-section of radius R_0 and a wall of small thickness h . The bent pipe axis is the flat curve $\Gamma_0 = \{x_0, y_0 : x_0 = x_0(s), y_0 = y_0(s)\}$ where s is an arc length. The pipe is immersed in a highly viscous medium and filled with a steady flow of a fluid, which is moving with velocity $g_{s,0}$ under the influence of a constant pressure drop. The geometry of the problem, the coordinate system and the general formulation of the problem are given in [3]. Below is the information necessary to understand the following text.

There are two coordinate systems: the global Cartesian coordinate system (O, x, y, z) and the curvilinear coordinate system (O, s, θ, R) . Curvilinear coordinates (O, s, θ, R) build on the currently axis Γ so that s is the length of the arc (OO') , and (O, θ, R) are the polar coordinates in the cross-section of a pipe. All equations of continuum mechanics are written below in curvilinear coordinates according to the methods of [10]. Formulas for all necessary geometrical parameters of the pipe axis and surface are derived in [4, 5].

For applicability of model equations, Vlasov's conditions [11] must be valid:

$$h^* = h / R_0 \leq 0.1; \min(L, \rho_0) / R_0 \geq 4.$$

The following parameter should be small:

$$\lambda = R_0 \max|\kappa_0(s)| \ll 1.$$

For the middle surface of the pipe's wall, the following geometric relationships are executed:

Copyright © 2019 for the individual papers by the papers' authors. Copyright © 2019 for the volume as a collection by its editors. This volume and its papers are published under the Creative Commons License Attribution 4.0 International (CC BY 4.0).

In: Sergey I. Smagin, Alexander A. Zatsarinnyy (eds.): V International Conference Information Technologies and High-Performance Computing (ITHPC-2019), Khabarovsk, Russia, 16-19 Sep, 2019, published at <http://eur-ws.org>

$$A = 1 + R_0 \kappa(s, t) \sin \theta, \quad B = R_0; \quad k_1 = \frac{\kappa(s, t) \sin \theta}{(1 + \kappa(s, t) R_0 \sin \theta)}, \quad k_2 = 1/R_0;$$

where k_1 and k_2 are the main curvatures of a median surface, κ is the axis curvature.

The equations of the three-dimensional mathematical model have next form (see [3, 9]).

For fluid movement:

$$\rho_f (v_0, \nabla) v_0 = -\nabla p - \bar{\Phi}(\mathcal{G}_{s_0}), \quad (\nabla, v_0) = 0, \quad \rho_f = \text{const.} \quad (1)$$

$$\Phi(\mathcal{G}_{s_0}) = \beta \mathcal{G}_{s_0}^2, \quad \beta = \frac{\lambda_1 \rho_f}{4R_0}, \quad Re = \frac{2\mathcal{G}_{s_0} R_0}{v_f}, \quad v_f = \mu_f / \rho_f;$$

$$\begin{cases} \lambda_1 = \frac{64}{Re}, & Re < 2000; \\ \lambda_1 = 0.0032 + \frac{0.221}{Re^{0.237}}, & Re \geq 2000. \end{cases}$$

For pipe wall movement in a shell approximation:

$$\begin{aligned} & \frac{1}{A} \frac{\partial I^{(0)}}{\partial s} - \frac{1-\nu}{B} \frac{\partial \chi_0}{\partial \theta} + (1-\nu) \left(k_1 k_2 u - \frac{k_2}{A} \frac{\partial w}{\partial s} \right) = -\frac{1-\nu^2}{Eh} X, \\ & \frac{1}{B} \frac{\partial I^{(0)}}{\partial \theta} + \frac{1-\nu}{A} \frac{\partial \chi_0}{\partial s} + (1-\nu) \left(k_1 k_2 v - \frac{k_1}{B} \frac{\partial w}{\partial \theta} \right) = -\frac{1-\nu^2}{Eh} Y, \\ & -(k_1 + k_2) \cdot I^{(0)} + \frac{1-\nu}{AB} \left[2ABk_1 k_2 w + \frac{\partial}{\partial s} (Bk_2 u) + \frac{\partial}{\partial \theta} (Ak_1 v) \right] - \frac{h^2}{12} \nabla^2 \nabla^2 w - \\ & - \frac{h^2}{12} \nabla^2 \left[(k_1^2 + k_2^2) w \right] = -\frac{1-\nu^2}{Eh} Z; \\ & \nabla^2 = \frac{1}{AB} \left[\frac{\partial}{\partial s} \left(\frac{B}{A} \cdot \frac{\partial \cdot}{\partial s} \right) + \frac{\partial}{\partial \theta} \left(\frac{A}{B} \cdot \frac{\partial \cdot}{\partial \theta} \right) \right]; \\ I^{(0)} &= \frac{1}{A} \left(\frac{\partial u}{\partial s} + \frac{A}{R_0} \frac{\partial v}{\partial \theta} + \nu \kappa \cos \theta \right) + \frac{1}{A} \left(\frac{A}{R_0} + \kappa \sin \theta \right) w - \frac{1}{2A^2} \left[\left(\frac{\partial w}{\partial s} \right)^2 + \left(\frac{\partial v}{\partial s} \right)^2 \right], \\ \chi_0 &= \frac{1}{2AB} \left[\frac{\partial}{\partial s} (Bv) - \frac{\partial}{\partial \theta} (Au) \right]; \quad \Phi_t(\mathcal{G}_{s_0}) = \frac{R_0}{2} \beta \mathcal{G}_{s_0}^2. \\ \frac{1}{h} X &= -\rho_t \frac{\partial^2 u}{\partial t^2} + \frac{1}{h} \Phi_t(\mathcal{G}_{s_0}), \quad \frac{1}{h} Y = -\rho_t \frac{\partial^2 v}{\partial t^2} - \frac{2\mu u^* \cos \theta}{hR_0 \left(0.5 - \ln \left| \frac{\gamma \rho_e u^*}{4 \mu} R_0 \right| \right)}, \\ \frac{1}{h} Z &= -\rho_t \frac{\partial^2 w}{\partial t^2} + \frac{1}{h} (p - p_e), \quad p_e = \rho_e g h_0 \left(1 - \frac{R_0}{h_0} \cos \theta \right) + \frac{2\mu u^* \sin \theta}{R_0 \left(0.5 - \ln \left| \frac{\gamma \rho_e u^*}{4 \mu} R_0 \right| \right)}. \end{aligned} \quad (2)$$

Here denoted: u, v, w are displacements of the median surface of a pipe along the coordinates s, θ, R , respectively; $I^{(0)}, \chi_0$ are first invariant of the strain tensor and the linear torsion of the pipe wall, respectively; X, Y, Z are components of the density of forces acting on the shell along the coordinates s, θ, R , respectively. For fluid: ρ_f is fluid density inside the pipe; μ_f is fluid viscosity; v_s, v_θ, v_R are components of the fluid velocity vector v_0 along the coordinate axes s, θ, R , respectively. For external pressure: $\gamma = 1.7811$ - number of Euler-Maskeroni; ρ_e is density of the medium; μ is viscosity of medium; h_0 is depth of immersion of the pipeline; u^* is velocity of the pipeline's cross-section motion. Equations (2) and the formulas for χ_0, ∇^2 are known from the shell theory by V.Z. Vlasov [11].

The system of equations (2) is supplemented by the boundary conditions of rigid fixing and by the homogeneous initial conditions:

$$\begin{aligned} u = 0, v = 0, w = 0, \quad \frac{\partial w}{\partial s} = 0 \quad \text{at } s = 0, s = L \text{ and any } t; \\ u = 0, v = 0, w = 0; \quad \frac{\partial u}{\partial t} = 0, \frac{\partial v}{\partial t} = 0, \frac{\partial w}{\partial t} = 0 \quad \text{at } t = 0. \end{aligned} \quad (3)$$

Boundary conditions for the equations of fluid flow (1):

$$v_s(0, \theta, R) = \mathcal{G}_{s_0}, \quad v_r(\zeta, \theta, R_0) = 0, \quad p(L, \theta, R) = p_a. \quad (4)$$

3 Applying Transformation Algorithm to Mathematical Model

We introduce dimensionless variables: $\zeta = s / \ell$, $r = R / R_0$, $\theta = \theta$, $\tau = \omega t$. Similarly, we do for unknown functions: $u' = u / R_0$, $v' = v / R_0$, $w' = w / R_0$; $v'_s = v_{s0} / \omega \ell$, $v'_\theta = v_{\theta 0} / \omega \ell$, $v'_r = v_{r0} / \omega \ell$, $p' = p / p_a$, $L' = L / \ell$.

The appropriate dimensionless unknown functions are presented as follows:

Velocity and pressure in fluid:

$$\begin{aligned} v'_s(\zeta, \theta, r) &= v_s^{(0)}(\zeta, r) + \lambda v_s^{(1)}(\zeta, r) \sin \theta + \lambda v_s^{(2)}(\zeta, r) \cos \theta + O(\lambda^2), \\ v'_\theta(\zeta, \theta, r) &= v_\theta^{(0)}(\zeta, r) + \lambda v_\theta^{(1)}(\zeta, r) \sin \theta + \lambda v_\theta^{(2)}(\zeta, r) \cos \theta + O(\lambda^2), \\ v'_r(\zeta, \theta, r) &= v_r^{(0)}(\zeta, r) + \lambda v_r^{(1)}(\zeta, r) \sin \theta + \lambda v_r^{(2)}(\zeta, r) \cos \theta + O(\lambda^2), \\ p'(\zeta, \theta, r) &= p^{(0)}(\zeta, r) + \lambda p^{(1)}(\zeta, r) \sin \theta + \lambda p^{(2)}(\zeta, r) \cos \theta + O(\lambda^2). \end{aligned} \quad (5)$$

The displacements of the median surface of a pipe wall:

$$\begin{aligned} u'(\zeta, \theta, \tau) &= u_0(\zeta) + \lambda u_1(\zeta, \tau) \sin \theta + O(\lambda^2); \\ v'(\zeta, \theta, \tau) &= \lambda v_1(\zeta, \tau) \cos \theta + O(\lambda^2); \\ w'(\zeta, \theta, \tau) &= w_0(\zeta) + \lambda w_1(\zeta, \tau) \sin \theta + O(\lambda^2). \end{aligned} \quad (6)$$

By means of (5), (6), the task is reduced to a one-dimensional problem.

Substitute the expressions (5), (6) into the three-dimensional problem (1)–(4). We obtain a reduced problem of the dynamics of the pipeline (see [9]):

$$\alpha^2 \frac{\partial^2 u_0}{\partial \zeta^2} + \nu \alpha \frac{\partial w_0}{\partial \zeta} - \alpha^3 \left(\frac{\partial w_0}{\partial \zeta} \frac{\partial^2 w_0}{\partial \zeta^2} \right) = -\frac{1}{E^* h^*} \frac{\alpha}{2} \ell \beta g_{s0}^2, \quad (7)$$

$$w_0 + \frac{h^{*2}}{12} \left(\alpha^2 \frac{\partial^2 w_0}{\partial \zeta^2} + \alpha^4 \frac{\partial^4 w_0}{\partial \zeta^4} \right) + \nu \alpha \frac{\partial u_0}{\partial \zeta} - \frac{\alpha^2}{2} \left(\frac{\partial w_0}{\partial \zeta} \right)^2 = \frac{1}{E^* h^*} [p_a + \ell \beta g_{s0}^2 (L' - \zeta) - \rho_e g h_0]. \quad (8)$$

$$\begin{aligned} \alpha^2 \frac{\partial^2 u_1}{\partial \zeta^2} - \frac{1-\nu}{2} u_1 - \frac{1+\nu}{2} \alpha \frac{\partial v_1}{\partial \zeta} + \nu \alpha \frac{\partial w_1}{\partial \zeta} + f \left[\frac{1-\nu}{2} u_0 - 2\alpha^2 \frac{\partial^2 u_0}{\partial \zeta^2} + \alpha(1-\nu) \frac{\partial w_0}{\partial \zeta} \right] - \\ - \alpha^3 \left(\frac{\partial w_1}{\partial \zeta} \frac{\partial^2 w_0}{\partial \zeta^2} + \frac{\partial w_0}{\partial \zeta} \frac{\partial^2 w_1}{\partial \zeta^2} \right) + 3\alpha^3 f \cdot \frac{\partial w_0}{\partial \zeta} \frac{\partial^2 w_0}{\partial \zeta^2} = \frac{\rho_t R_0^2 \omega^2}{E^*} \frac{\partial^2 u_1}{\partial \tau^2}; \end{aligned} \quad (9)$$

$$\begin{aligned} \frac{1-\nu}{2} \alpha^2 \frac{\partial^2 v_1}{\partial \zeta^2} - v_1 - \frac{1}{E^* h^*} \frac{2u_1^* \mu}{R_0 \left(0.5 - \ln \left| \frac{\nu \rho_e \lambda u_1^*}{4\mu} R_0 \right| \right)} + \frac{1+\nu}{2} \alpha \frac{\partial u_1}{\partial \zeta} + \\ + w_1 + f \left(w_0 - \frac{3-\nu}{2} \alpha \frac{\partial u_0}{\partial \zeta} \right) - \alpha^2 \frac{\partial w_0}{\partial \zeta} \frac{\partial w_1}{\partial \zeta} = \frac{\rho_t R_0^2 \omega^2}{E^*} \frac{\partial^2 v_1}{\partial \tau^2}; \end{aligned} \quad (10)$$

$$\begin{aligned} w_1 + \frac{h^{*2}}{12} \left(\alpha^4 \frac{\partial^4 w_1}{\partial \zeta^4} - \alpha^2 \frac{\partial^2 w_1}{\partial \zeta^2} \right) + \nu \alpha \frac{\partial u_1}{\partial \zeta} - v_1 + f \left[2\nu w_0 + (1-\nu) \alpha \frac{\partial u_0}{\partial \zeta} \right] - \alpha^2 \frac{\partial w_0}{\partial \zeta} \frac{\partial w_1}{\partial \zeta} + \frac{\alpha^2}{2} f \left(\frac{\partial w_0}{\partial \zeta} \right)^2 = \\ = \frac{1}{E^* h^*} \left[\rho_f g_{s0}^2 f - \frac{2u_1^* \mu}{R_0 \left(0.5 - \ln \left| \frac{\nu \rho_e \lambda u_1^*}{4\mu} R_0 \right| \right)} \right] - \frac{\rho_t R_0^2 \omega^2}{E^*} \frac{\partial^2 w_1}{\partial \tau^2}. \end{aligned} \quad (11)$$

As shown in [9], the solution of the problem on fluid dynamics and the solution of the zero-approximation problem (7), (8) can be considered known. The boundary conditions for the system of the first approximation equations (9)–(11) have the form:

$$\begin{aligned} v_1 = w_1 = 0, \quad \frac{\partial w_1}{\partial \zeta} = 0 \quad \text{at } \zeta = 0, \zeta = L' \text{ and any } \tau; \\ u_1 = v_1 = w_1 = 0, \quad \frac{\partial u_1}{\partial \tau} = \frac{\partial v_1}{\partial \tau} = \frac{\partial w_1}{\partial \tau} = 0 \quad \text{at } \tau = 0 \text{ and any } \zeta. \end{aligned} \quad (12)$$

The difference scheme for solving the initial-boundary value problem (9)–(12) is described in the article [9]. From expressions (6), it follows that the physical sense of $\lambda u_1 R_0$ is a displacement of points from the cross-sectional plane perpendicular to the axial line of the pipe, i.e., warping [1]. Sectional warping of the cross-section of a cylindrical pipe was observed in the experiments of V.Z. Vlasov in [12].

4 Numerical Experiments for Mechanical Problems

Task 1. Cubic parabola $y = 10^{-8}x(x - 6000)(x - 12000), 0 \leq x \leq 12000$. Values of the main geometrical parameters: $L = 12500 \text{ m}$, $\min|\rho_0| \approx 3951.5 \text{ m}$. Uniform current velocity $\vartheta_{s_0} = 1 \text{ m/s}$ calculated over the interval of time $T_{end} = 864000 \text{ s}$ or 10 days.

Task 2. Fractional-rational function $y = 40(1 - 0.001x)/(1 + 10^{-6}x^2), -6000 \leq x \leq 6000$. Values of the main geometrical parameters: $L = 12000 \text{ m}$, $\min|\rho_0| \approx 1194.5 \text{ m}$. Uniform current velocity $\vartheta_{s_0} = 1 \text{ m/s}$ calculated interval of time $T_{end} = 691200 \text{ s}$ or 8 days.

Other parameters are equal: $\rho_e = 1700 \text{ kg/m}^3$, $\mu = 10000 \text{ N}\cdot\text{s/m}^2$, $\rho_t = 7200 \text{ kg/m}^3$, $h = 0.005 \text{ m}$, $E = 2.07 \cdot 10^{11} \text{ N/m}^2$, $\nu = 0.24$, $R_0 = 0.3 \text{ m}$, $\mu_f = 0.667 \text{ N}\cdot\text{s/m}^2$, $\rho_f = 850 \text{ kg/m}^3$.

Figure 1 shows the coordinates of the pipeline profile and its warping in task 1.

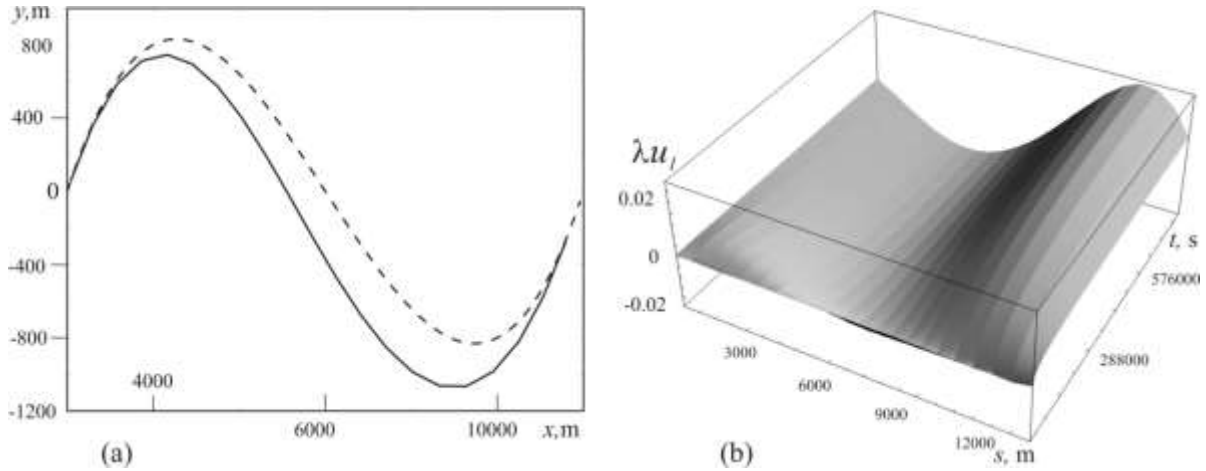


Figure 1: (a) – the profile coordinates at the start (dashed line) and at the calculation end; (b) – the longitudinal displacement in a first approximation.

Displacements of the axial line shown in Figure 1 (a), illustrate the coherence of the numerical calculations for the offered mathematical model with the fundamental laws of mechanics. The existence of the cross-sectional warping is confirmed by the graph of the longitudinal wall displacements in Figure 1 (b), the geometric meaning of which is the warping of the cross-section. Thus, the numerical experiment indicated the existence of the cross-sectional warping of the long thin-walled pipeline of the order $0.02R_0$.

In Figure 2, the coordinates of a profile of the pipeline and warping of cross-sections in task 2 are represented. Similar to task 1, the change in the coordinates of the profile at the start (dotted line) and at the end of the calculation in Figure 2 (a) indicates the coherence of the numerical experiment with the laws of mechanics. Cross-sectional warping also occurred in this case, with a warping on the order of $0.003R_0$, as shown in Figure 2 (b).

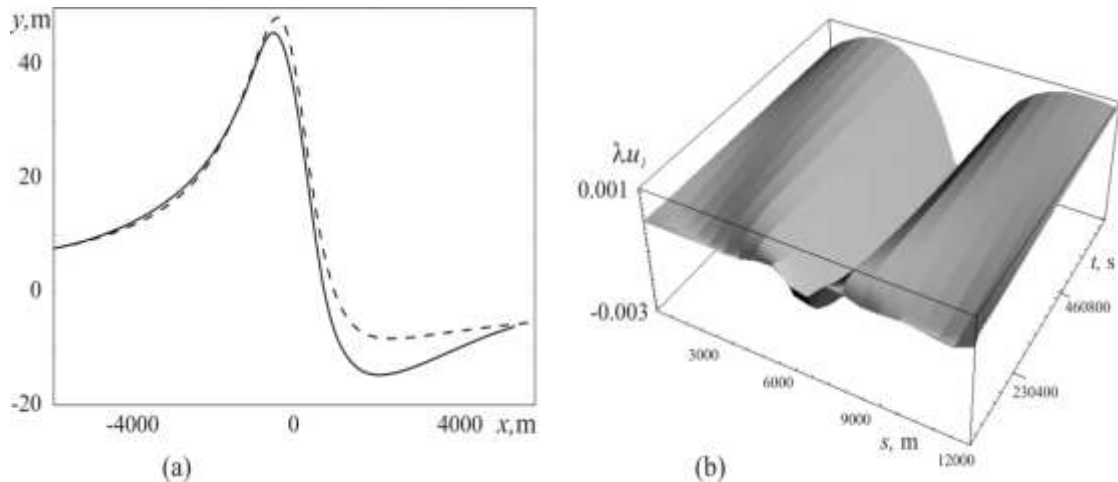


Figure 2: (a) – the profile coordinates at the start (dashed line) and at the calculation end; (b) – the longitudinal displacement in a first approximation.

5 The Pipeline Displacements under the Dynamic Pressure Action

In tasks above, the pressure difference is considered to be constant on the ends of a pipe, which enabled the constant velocity of an internal stream of fluid. For all tasks, numerical experiments were conducted in which the pressure difference changed under the piecewise linear law:

$$\Delta p = \begin{cases} \Delta p_0, & t \leq t_0; \\ \Delta p_0 \left[k_p + \frac{k_p - 1}{\Delta t} (t - t_0 - \Delta t) \right], & t_0 < t < t_0 + \Delta t; \\ k_p \Delta p_0, & t_0 + \Delta t \leq t \leq t_1 - \Delta t; \\ \Delta p_0 \left[1 + \frac{k_p - 1}{\Delta t} (t_1 - t) \right], & t_1 - \Delta t < t < t_1; \\ \Delta p_0, & t \geq t_1. \end{cases}$$

Here, Δp_0 is the pressure difference providing the flow velocity g_{s0} ; t_0, t_1 – time of the beginning and of the ending of a pressure's jump, respectively; Δt – time during which the pressure changes; and k_p is factor of the pressure's increase. The initial pressure drop is determined by the formula for the hydraulic resistance of the pipe (see [13]):

$$\Delta p_0 = \lambda_1 \frac{L}{4R_0} \rho_f g_{s0}^2,$$

with the other parameters set by the formulation of the numerical experiment.

In the example shown here, $T_{end} = 1209600$ s or 14 days; $k_p = 1.5$; $t_0 = 86400$ s, $t_1 = 360000$ s or 4 days; $\Delta t = 2$ hours. The results of the displacement calculation and the centreline's coordinates are shown in Figure 3.

Figure 3 shows a part of a movement's 3D-graph over a duration of 125 hours. In the graph, the time interval in which the influence of the pressure jump leading to an increase in the deflection is expressed is detached. Next, according to the decrease in the pressure, the pipe returns to the position corresponding to the position of the final equilibrium of task 2.

In Figure 3 (b), the coordinates of the axial line at the beginning of the calculation, at the moment of time corresponding to the strongest deviation of a profile and at the final moment of time are shown. It was established that the slowly varying pressure difference eventually leads to the same steady state as the constant pressure difference, provided that the final values of the differences are equal.

6 Conclusion

We presented the new mathematical model of dynamics of the curvilinear pipeline on the basis of the shells theory. A method for the approximate solution of the model equations based on the asymptotic expansion of the solution was proposed. Results of numerical experiments for model problems were given. It was proved that the mathematical model adequately describes the known phenomena of pipelines mechanics. In the numerical experiment, the deplanations of the pipe cross sections were found. It is shown that the mathematical model is applicable in the case of a slow change in the internal pressure in a fluid.

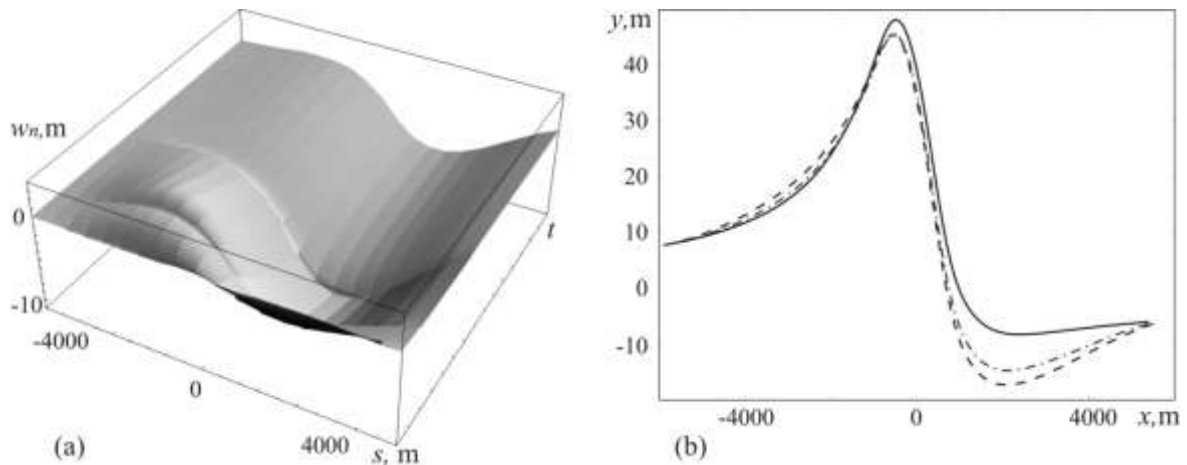


Figure 3: (a) - normal displacements of the axial line; (b) - coordinates of the axial line for $t = 10$ minutes (the continuous line), $t = 4$ days (dotted line), and $t = 14$ days (dot-dash line).

Acknowledgements

This research was supported in through computational resources provided by the Shared Facility Center “Data Center of FEB RAS” (Khabarovsk).

References

1. Feodosiev, V.I.: *Advanced Stress And Stability Analysis: Worked Examples*, Springer, Berlin, Heidelberg (2005)
2. Towhata, I.: *Geotechnical Earthquake Engineering*, Springer, Berlin, Heidelberg (2008)
3. Rukavishnikov, V.A., Tkachenko, O.P.: Dynamics of a fluid-filled curvilinear pipeline, *Applied Mathematics and Mechanics (English Edition)*. 39 (6): 905–922 (2018)
4. Tkachenko, O.P.: Construction of the Mathematical Model of Complex Pipeline with Variable Geometry, *Procedia Engineering*. 165: 1261–1274 (2016)
5. Rukavishnikov, V.A., Tkachenko, O.P.: Numerical and Asymptotic Solution of the Equations of Propagation of Hydroelastic Vibrations in a Curved Pipe, *J. Appl. Mech. Tech. Phys*: 41 (6): 1102–1110 (2000)
6. Rukavishnikov, V.A., Tkachenko, O.P.: Nonlinear equations of motion of an extensible underground pipeline: derivation and numerical modeling, *J. Appl. Mech. Tech. Phys*: 44 (4): 571–576 (2003)
7. Rukavishnikov, V.A., Tkachenko, O.P.: Effect of the pipe curvature on internal elastic wave propagation, *Computational Mathematics and Mathematical Physics*. 50 (11): 1886–1894 (2010)
8. Rukavishnikov, V.A., Tkachenko, O.P.: Numerical analysis of the mathematical model of hydroelastic oscillations in a curved pipeline, *Mathematical Models and Computer Simulations*: 3 (4): 508–516 (2011)
9. Rukavishnikov, V.A., Tkachenko, O.P.: Approximate solution to the nonlinear problem of an underground pipeline deformation, *Journal of Applied and Industrial Mathematics*: 6 (1): 100–110 (2012)
10. Sedov, L.I.: *A Course in Continuum Mechanics*. Translation from the Russian, ed. by J.R.M. Radok, Wolters-Noordhoff Publishing, Groningen (1972)
11. Vlasov, V.Z.: *Basic Differential Equations in General Theory of Elastic Shells*, National Advisory Committee for Aeronautics, NACA-TM-1241, (1951), <https://ntrs.nasa.gov/search.jsp?R=20050028489>
12. Vlasov, V.Z.: The general principles of construction of the technical theory of shells, In: Vlasov V.Z. *Selected works*. V.2. RAS, Mocsow: 467–503 (1963) (in Russian)
13. Loitsyanskii, L.G.: *Mechanics of Liquids and Gases*, Pergamon Press, Oxford, New York (1966)